



Research paper

Sources and health risk assessment of potentially toxic elements in groundwater in the mineral-rich tribal belt of Bastar, Central India



Shamsh Pervez^{a,*}, Princy Dugga^a, Mohammad Nahid Siddiqui^b, Shahina Bano^a,
Madhuri Verma^a, Carla Candeias^c, Archi Mishra^a, Sushant Ranjan Verma^a,
Aishwaryashri Tamrakar^a, Indrapal Karbhal^a, Manas Kanti Deb^a, Kamlesh Shrivastava^a,
Yasmeen Pervez^d, Rakesh Kumar Jha^e

^a School of Studies in Chemistry, Pt. Ravishankar Shukla University, Raipur, 492010, Chhattisgarh, India

^b Department of Chemistry and IRC Membranes and Water Security, King Fahd University of Petroleum & Minerals, Dhahran, Saudi Arabia

^c GeoBioTec, Geosciences Department, University of Aveiro, Aveiro Santiago Campus, Portugal

^d Government Eklavya College, Dondi Lohara, Chhattisgarh, India

^e Thermo Fischer Scientific, Powai, Mumbai, 400076, India

ARTICLE INFO

Keywords:

Groundwater

Potentially toxic element

Carcinogenic risk

Principal component analysis

Positive matrix factorization

ABSTRACT

Concentrations of trace elements (Al, B, As, Be, Cd, Ba, Co, Cu, Fe, Cr, Sb, Ni, Li, Sn, Mn, Zn, V and Se) were determined in 160 groundwater samples, collected during pre-monsoon (PRM) and post-monsoon (POM) period (2017) in the tribal belt of Bastar, central India, using inductive coupled plasma mass spectrometry (ICP-MS). The concentrations of Al, As, Fe, Mn and Ni were found exceeding the permissible limits in 49% of samples. Cd, Sn and Se elements have shown two-fold increment in POM samples than those collected during PRM. On the contrary, Al, Ba, Co, Cr and Fe have shown a declining trend from PRM to POM period. On applying Principal component analysis (PCA) and Positive matrix factorization (PMF) approaches to the dataset, observed three primary sources (natural, geogenic and agricultural) for groundwater elemental components. Among the measured potentially toxic elements (PTEs), As has shown higher carcinogenic and non-carcinogenic risk in children as well as adults. This study recommends the regular monitoring of heavy metal contamination of groundwater as various geogenic and anthropogenic activities may elevate the risk of severe health hazards.

1. Introduction

Worldwide, 71% of the population access clean drinking water while 844 million people across the world still lack clean drinking water. This issue is more severe in rural areas where only one out of three people use safe drinkable water (WHO, 2019). In India, most rural and suburban regions rely on groundwater to meet water demand for drinking and domestic purposes (Clark et al., 1996; Ahada and Suthar 2018).

Among all contaminants, inorganic trace elements are of much concern as they are xenobiotic compounds and can accumulate in the water resources for a long period (Ravindra and Mor 2019). Groundwater has the potential to accumulate trace elements that reach the water table and pollute it through various natural and anthropogenic sources such as precipitation, rock-water interaction, percolation of soil-water, industrial wastewater, agricultural, domestic wastes, etc.

(Boateng et al., 2016; Bouderbala and Gharbi 2017; Hossain and Patra 2020).

However, depletion in water quality is related to public health concerns, so it is essential to estimate the exposure risk to understand groundwater sources' toxicity level imposing health hazards. Trace metals in groundwater may be exposed to human beings through two key pathways, direct ingestion and dermal absorption (Duggal and Rani 2018; Brindha et al., 2020; Hu et al., 2020). Some trace metal(loid)s such as arsenic (As), lead (Pb), nickel (Ni), chromium (Cr), copper (Cu), zinc (Zn), cadmium (Cd), and cobalt (Co) are potentially toxic if found above their threshold value in drinking water (Islam et al., 2019; Hossain and Patra 2020). Lead can cause neurological diseases as it can trigger the central nervous system mostly in children which results in fatigue, anaemia, and a decrease in intelligence quotient (IQ) level (Emenike et al., 2019). Cadmium excess affects renal function and can

* Corresponding author.

E-mail address: shamshpervez@gmail.com (S. Pervez).

<https://doi.org/10.1016/j.gsd.2021.100628>

Received 20 March 2021; Received in revised form 13 June 2021; Accepted 14 June 2021

Available online 19 June 2021

2352-801X/© 2021 Elsevier B.V. All rights reserved.

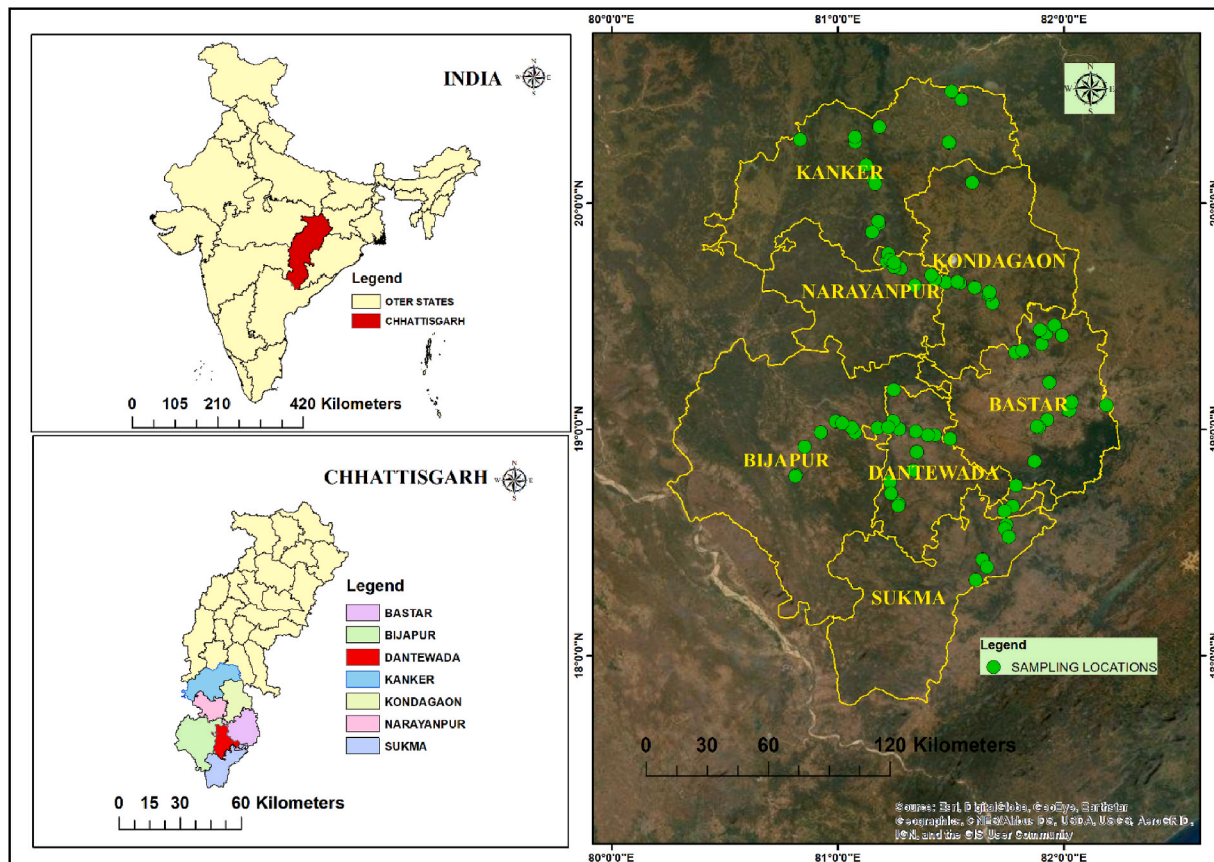


Fig. 1. Map of groundwater sampling locations across the Bastar region.

induce severe kidney diseases and even cancer. Consumption of water with high concentrations of arsenic can cause cardiovascular, neurological, and skin diseases such as hyperpigmentation, hyperkeratosis and can develop cancer (Emenike et al., 2019). Pandey et al. (2015) have reported higher As contamination in the groundwater of Kanker district (India) and carried out an epidemiological investigation reporting sub-acute As poisoning that resulted in gastrointestinal disease diarrhoea in inhabitants of the study area.

Previously very few studies on the evaluation of groundwater contamination have been reported for the study region and all of those studies were mainly focused on reporting selected major constituents and few toxic elements for a small number of location (Behera et al., 2012; Rubina and Kavita, 2013; Pandey et al., 2015). Source apportionment of trace elements, including potentially toxic species in groundwater allows to address the relative contribution from different major source routes viz. geogenic, anthropogenic (e.g., agricultural), and atmospheric (re)suspended materials, and studies that relate these results to assess health risks are scarce for the tribal belt of Bastar region. Thus, investigation of the potential source of groundwater contaminants, particularly potentially toxic trace elements and associated health risks is mandatory. Further this study aims to, 1) evaluate the spatio-temporal variations in trace element concentrations in groundwaters during pre-monsoon (PRM) and post-monsoon (POM) periods; 2) identify the significant sources of groundwater contamination using Principal Component Analysis (PCA) and chemical mass balance approach through positive matrix factorization (PMF); and 3) assess health risk caused by potentially toxic elements (PTEs).

2. Materials and methods

2.1. Study area

Sampling was performed at ninety-five locations across the seven districts of the Bastar division (80° 35'E – 82° 15'E and 17° 46' N-20° 35'N). QGIS 3.14 software was used to make a detailed map of the study area (Fig. 1).

Bastar region is considered a mineral-rich area of the Chhattisgarh state (India). Geologically, the study area is located on the Bastar Craton, with an ~215,000 km² extension, mainly composed of gneisses, granitoid, granulites, supracrustals, and mafic igneous rocks, being these last ones exposed in diverse locations, along with dykes characterized with a high-Mn and high-Fe quartz tholeiitic composition (Dora, 2014). The lithology of the study area is characterized by gneiss granitoids, meta-sediments in the Sukma region (Bengal), Bhopalpatnam, Kondagaon and Balaghat granulites, Bailadila Iron Formation, Dongargarh and Kotri Supergroup that includes the Dongargarh- Malajkhand and equivalent granitoids, the Sauser and Sonakhan Group of rocks and the platform sediments of Purana basins, among others. Soils are mainly vertisol and alfisol, these last ones with origin in the cratonic rocks (Gupta et al., 2012). Limestones and bauxites are common in this region, with Fe and Ti enrichment (Mineral Resource Department, 2014).

The study region is mainly drained by the Indravati and Sabri rivers which are tributaries of the Godavari River. It constitutes the agro-climatic region with sandy to clayey soil structure with considerable variation in soil types such as laterite, alluvial and loamy soil (Sinha, 2011). The total irrigated area in this region is 12,085 ha while the net sown area covers 6,37,965 ha (Department of Land Resource Management, 2014). The total forest area of the Bastar region is 7112 km², accounting for more than 75% of its land area (Sinha, 2011). The annual temperature variation ranges between 10° C to 46° C and the annual

rainfall across the Bastar region is in mean ~ 1387 mm. Precipitation occurs in this region due to the southwest monsoon attributed to the Bay of Bengal during June–September. Groundwater aquifers mostly arise in phreatic and semi-confined conditions.

2.2. Sampling and chemical analysis

The representative 160 groundwater samples were collected during pre and post-monsoon season out of which 65 samples were collected in the Pre-monsoon season (50 bore wells+15 Dug wells) while in post-monsoon season 95 samples were collected (72 bore wells+23 dug wells) using the stratified random sampling method applying pooled study design. The stagnant water of the column was pumped out for at least 10 min before sampling. For heavy metal analysis, water samples were filtered using Whatman 42 filter papers and immediately acidified with concentrated HNO_3 acid ($\text{pH} < 2$). AR grade acids and reagents were used in the study. Each sampling bottle was rinsed with the sampled groundwater before collection. Physical parameters such as pH, electrical conductivity (EC), total dissolved solids (TDS), and temperature (T) were measured in situ using HANNA® sensors (HI 98129) (Varghese and Jaya 2014; Guo et al., 2017). Water samples were filled up to the bottle's rim and were sealed tightly to prevent exposure to air. Samples were placed in an icebox and carefully transported to the laboratory and stored in a deep freezer (-4°C) for further analysis.

2.3. Chemical analysis

Selected trace elements (Al, B, As, Be, Cd, Ba, Co, Cu, Fe, Cr, Sb, Ni, Li, Sn, Mn, Zn, V, and Se) were analyzed in groundwater samples using inductively coupled plasma mass spectrometry (ICP-MS; ThermoFischer, Model iCAP RQ.ASX-560). Thermo Scientific Qtegra Intelligent Scientific Data Solution (ISDS) software was used for operating the instrument. Helium gas flow rate was set at 4.5 mL min^{-1} , while nebulizer argon flow rate was 1.14 min^{-1} and the integration time was set at 0.02 s per point for analysis. The internal standards (Sc, Tl, Ge, In, and Bi) with the known concentrations of 0.1, 0.5, 1, 10 and $50 \mu\text{g L}^{-1}$ were used for calibration purposes. Samples were pre-treated with 0.1 N HNO_3 acid and internal standards. Replicate measurements were carried out for all trace elements to maintain the relative standard deviation within 10%. The recovery percentage of the heavy metal/metalloids ranged between 76 and 98% indicating a good correlation between the actual and measured values.

2.4. Quality control

Quality control was obtained by applying standard laboratory measures and quality assurance strategies were applied during analysis such as replicate measurement of samples, use of analytical grade reagents and chemicals, and by adopting standard operational procedures of sample analysis. Throughout the analysis reagent blank, metal concentration, and its standard detection limits were observed.

2.5. Data compilation and statistical methods

The spatial variability of trace elements across the monitoring locations was calculated by dividing the standard deviation with the mean value of chemical species and taking its percentage and designated it as the coefficient of spatial variation (% CV). Source signatures of groundwater chemical components were determined using the PCA technique using IBM SPSS® 22 statistic software. The quantification of source contribution estimates of groundwater contaminants was carried out by executing USEPA PMF 5.0 using concentrations and associated analytical uncertainties of trace elements (US-EPA, 2014). Reported concentrations of groundwater ionic species (Dugga et al., 2020) were also included in the chemical input profiles of groundwater samples during the execution of PMF5.0 for evaluating more precise and

appropriate results of source apportionment.

3. Human health risk assessment

3.1. Exposure assessment

The exposure assessment estimates the magnitude and potential concerning chemical exposure to individuals, considering the pathways through which chemicals are usually transported and the major routes by which an individual is exposed to chemicals (USEPA, 2004). To evaluate the health risk impact posed by each element, USEPA (2004) risk assessment protocol was used. Due to the distinct behavior, exposure dose and body weight, health risk assessment was calculated for the two age groups: children (0–15 years) and adults (>15 years) (USEPA, 2011). Exposure to potentially toxic elements (PTEs) present in groundwater can occur via two major exposure pathways: (a) ingestion via drinking water intake through the mouth; and (b) dermal contact (Prasanth et al., 2012; Li et al., 2016). Daily exposure and health risk assessment were evaluated for nineteen trace elements (Al, As, B, Ba, Be, Cd, Co, Cr, Cu, Fe, Li, Mn, Ni, Sb, Se, V, Zn, F^- and NO_3^-) associated with the groundwater using: (i) chemical daily intake (CDI) which account for direct ingestion via drinking water intake (Liu et al., 2020) (Eq. (1)); and (ii) dermal absorbed dose (DAD) which accounts for the dermal absorption of PTEs adhered to skin (Eq. (2))

$$CDI = \frac{C \times IR \times EF \times ED}{BW \times AT} \quad (1)$$

$$DAD = \frac{C \times SA \times Kp \times ET \times EF \times ED}{BW \times AT} \times CF \quad (2)$$

Where CDI and DAD are in $\text{mg.kg}^{-1} \text{ day}^{-1}$, C denotes the concentration of trace elements in mg.L^{-1} , IR is ingestion rate in mg.day^{-1} and EF is relative exposure frequency in days.year^{-1} , ED is exposure duration in years, BW is average body weight in kg, AT is the average time in days, SA denotes the exposed skin area (cm^2), Kp is coefficient of dermal permeability in cm.h^{-1} , ET is the exposure time (h.day^{-1}) and CF is the conversion factor (unitless) Factor values of each parameter used in the calculation of exposure assessment have been mentioned in Table 3.

3.2. Non-carcinogenic risk assessment

Risk assessment is described as the method of analyzing and determining the potential event that probably causes harmful health effects over a specific time duration and concludes the ability to tolerate risk based on risk analysis (EPA 1989; Mohammadi et al., 2019). In this study, non-carcinogenic risk assessment was evaluated using hazard quotient (HQ) and hazard index (HI) expressed as

$$HQ_{ing} = \frac{CDI}{RfD} \quad (3)$$

$$HQ_d = \frac{DAD}{RfD \times GIABS} \quad (4)$$

$$HI_i = HQ_{ing} + HQ_d \quad (5)$$

$$HI = \sum HI_i \quad (6)$$

Where HQ_{ing} and HQ_d are hazard quotient for oral ingestion and dermal exposure, respectively, RfD represents oral reference dose, GIABS denotes the gastrointestinal absorption factor, while the total non-carcinogenic risk was calculated as the summation of hazard quotient of oral and dermal exposure using hazard index (HI). HQ and HI values $< 1.00 \text{ E}+00$ considered safe while values $> 1.00 \text{ E}+00$ indicate that an individual is exposed to non-carcinogenic risk (Ravindra and Mor 2019; Yavar Ashayeri and Keshavarzi 2019).

Table 1

Descriptive statistics of trace and potentially toxic elements in the 160 groundwater samples, collected from Bastar region during Pre-Monsoon (PRM) and Post-monsoon (POM) periods.

Species	BIS Limit	WHO Limit	MDL values (ICPMS)	Pre- Monsoon					Post-Monsoon						
				Overall water samples (n = 73)		Dug Well (n = 20)		Bore Well(n = 53)		Overall water sample (n=87)		Dug Well (n = 18)		Bore Well (n = 69)	
				Geo mean ± SD (Min-Max)	Mean ± SD	%CV	Mean ± SD	%CV	Geo mean ± SD (Min-Max)	Mean ± SD	%CV	Mean ± SD	%CV		
Al	30	-	0.199	8.01 ± 21.60 (0.25-13.64)	17.49 ± 21.09	120.58	15.64 ± 21.97	140.47	5.82 ± 18.05 (0.79-94.06)	6.86 ± 4.36	63.67	12.45 ± 20.02	160.80		
As	10	10	0.003	7.22 ± 3.46 (1.02-20.03)	8.24 ± 2.20	26.69	8.20 ± 8.67	105.73	7.29 ± 2.57 (1.24-12.33)	8.37 ± 2.52	30.10	7.73 ± 2.59	33.50		
B	300	2400	0.123	10.56 ± 26.79 (0.25-135.64)	23.47 ± 27.22	115.98	19.92 ± 26.83	134.68	9.77 ± 24.38 (0.86-141.06)	9.70 ± 7.46	76.90	19.71 ± 26.78	135.87		
Ba	700	700	0.034	73.14 ± 132.81 (11.68-615.32)	83.99 ± 57.92	68.96	119.69 ± 151.14	126.27	67.75 ± 108.24 (0.03-759.29)	69.14 ± 41.01	59.31	109.64 ± 118.53	108.11		
Be	-	-	0.032	6.05 ± 14.92 (0.89-66.94)	12.82 ± 18.39	143.45	10.57 ± 13.53	128.00	6.24 ± 13.80 (0.35-65.96)	11.65 ± 14.87	127.63	10.63 ± 13.62	128.13		
Cd	3	3	0.023	0.03 ± 0.28 (0.001-0.99)	0.13 ± 0.30	230.77	0.14 ± 0.27	192.85	0.06 ± 0.27 (0.01-1.17)	0.13 ± 0.29	223.07	0.15 ± 0.26	173.33		
Co	-	-	0.002	1.61 ± 1.70 (0.06-6.52)	2.67 ± 1.61	60.30	2.27 ± 3.53	155.51	0.13 ± 0.84 (0.0005-6.97)	0.23 ± 0.24	104.16	0.42 ± 0.44	104.76		
Cr	50	50	0.003	1.79 ± 14.00 (0.16-60.34)	9.28 ± 15.13	163.04	8.14 ± 13.69	168.18	1.08 ± 9.10 (0.12-40.72)	4.75 ± 10.50	221.11	3.95 ± 4.76	120.51		
Cu	50	2000	0.036	2.15 ± 6.95 (0.14-30.43)	5.13 ± 8.94	174.27	4.28 ± 6.12	142.99	2.09 ± 7.25 (0.18-31.70)	5.31 ± 1.58	29.75	4.46 ± 7.02	157.39		
Fe	300	-	0.011	388.41 ± 374.29 (164.32-2023.76)	450.89 ± 316.73	70.25	491.25 ± 396.06	80.62	357.37 ± 405.90 (104.27-2353.81)	364.95 ± 232.01	63.57	471.08 ± 438.85	93.16		
Li	-	-	0.069	5.97 ± 25.65 (0.13-99.87)	15.10 ± 28.61	189.47	14.42 ± 24.73	171.49	6.76 ± 23.23 (0.18-97.78)	11.51 ± 22.94	199.30	15.14 ± 23.41	154.62		
Mn	100	-	0.006	145.57 ± 170.79 (52.49-823.89)	164.77 ± 104.99	63.72	202.09 ± 189.66	93.85	178.07 ± 338.07 (32.71-2090.03)	167.33 ± 52.17	31.18	270.71 ± 147.59	54.52		
Ni	20	-	0.007	2.88 ± 13.09 (0.140-53.10)	8.94 ± 15.18	169.80	7.82 ± 15.59	199.36	3.59 ± 7.79 (0.26-35.06)	9.15 ± 9.15	100.00	5.99 ± 7.33	122.37		
Sb	-	20	0.003	0.06 ± 0.30 (0.004-0.99)	0.21 ± 0.30	142.86	0.19 ± 0.31	163.16	0.05 ± 0.19 (0.01-0.91)	0.12 ± 0.22	183.33	0.11 ± 0.18	163.63		
Se	10	40	0.063	0.09 ± 0.44 (0.004-1.73)	0.30 ± 0.51	170.00	0.27 ± 0.42	155.55	0.19 ± 0.79 (0.004-3.98)	0.57 ± 0.92	161.40	0.47 ± 2.60	553.19		
Sn	-	-	0.009	0.03 ± 0.26 (0.001-0.99)	0.16 ± 0.32	200.00	0.13 ± 0.23	176.92	0.06 ± 0.22 (0.002-0.99)	0.12 ± 0.24	200.00	0.13 ± 0.21	161.53		
V	-	-	0.002	0.53 ± 10.91 (0.01-45.07)	4.91 ± 12.20	248.47	4.52 ± 10.51	232.52	0.85 ± 8.38 (0.03-35.04)	3.44 ± 8.62	250.58	4.55 ± 8.36	183.73		
Zn	5000	-	1.183	178.26 ± 275.49 (12.09-1538.75)	295.56 ± 234.76	79.43	281.35 ± 434.85	154.56	256.85 ± 427.55 (66.81-2612.25)	258.16 ± 151.00	58.49	397.32 ± 470.56	118.43		

All concentrations in $\mu\text{g.L}^{-1}$; MDL-Minimum detection limit ($\mu\text{g.L}^{-1}$); Geo mean – Geometric mean; SD – standard deviation; CV - coefficient of spatial variation.

3.3. Carcinogenic risk assessment

The potential carcinogenic risk (CR) represents the probability of developing cancer in an individual during lifetime exposure to carcinogenic elements (El Nemr et al., 2016; Yavar Ashayeri and Keshavarzi 2019). The carcinogenic risk was evaluated for two carcinogenic elements (As and Cr) using the following equations:

$$CR_{ing} = CDI \times SF_o \tag{7}$$

$$CR_d = DAD \times \left(\frac{SF_o}{GIABS} \right) \tag{8}$$

$$CR_i = CR_{ing} + CR_d \tag{9}$$

$$CR = \sum CR_i \tag{10}$$

Where CR_{ing} and CR_d represent carcinogenic risk by oral and dermal exposure, respectively, SF_o denotes oral slope factor ($\text{mg.kg}^{-1}.\text{day}^{-1}$)⁻¹ while CR is the total carcinogenic risk (Li et al., 2016). The CR value < 10⁻⁶ shows no significant risk, 10⁻⁶ to 10⁻⁴ considered tolerable, while values > 10⁻⁴ indicate a high carcinogenic risk.

4. Results and discussion

4.1. Groundwater chemical characterization

This study shows the concentration of eighteen trace elements in groundwater samples collected from the Bastar region during the PRM and POM periods of 2017. In addition to the tabulation of mean concentrations of the elemental species for all groundwater samples collected on the two periods, similar statistics were presented separately for dug-well and bore-well groundwater samples in Table 1. Further, these concentrations were used to evaluate the spatiotemporal variability, source apportionment, and health risk assessment to achieve a clear groundwater hydrochemistry scenario in the study area.

The abundance order based on the geometric mean (GM) value of trace elements concentration in overall groundwater samples of the study area were as follows: Fe > Zn > Mn > Ba > B > Al > As > Be > Li > Ni > Cu > Cr > Co > V > Se > Sb > Sn > Cd in PRM and Fe > Zn > Mn > Ba > B > As > Li > Be > Al > Ni > Cu > Cr > V > Se > Co > Sn > Cd > Sb in POM.

Among all the trace elements, the highest average concentration was obtained for Fe (GM: 388.40 ± 374.29 $\mu\text{g.L}^{-1}$ in PRM and GM: 357.37 ±

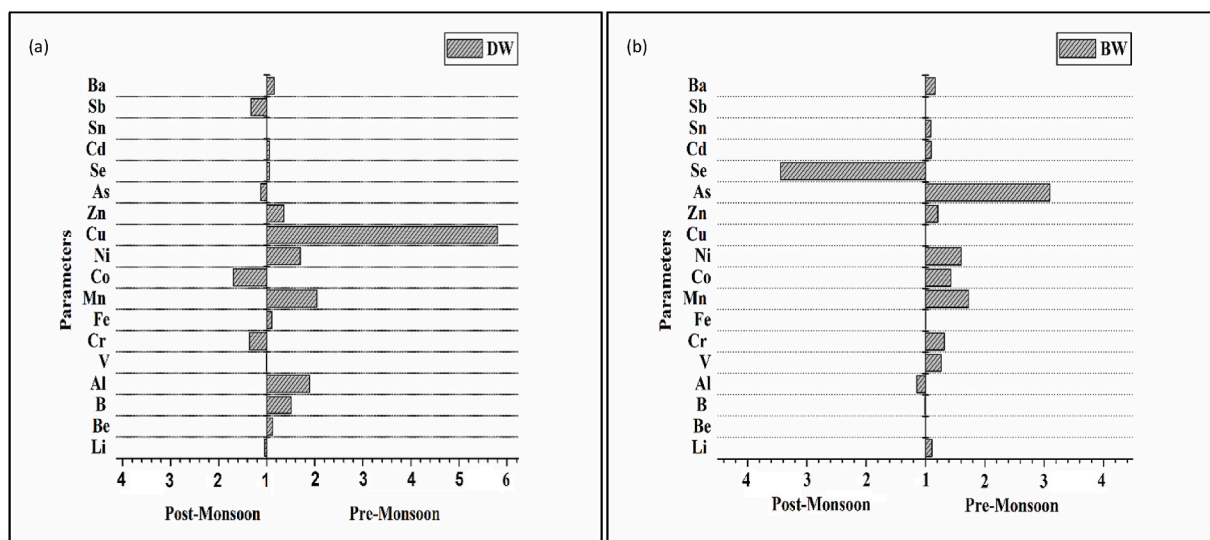


Fig. 2. Spatiotemporal variation trend shown by trace and toxic elements in (a) dug well (DW) and (b) borewell (BW) samples [(%CV) between pre and post-monsoon periods].

405.90 $\mu\text{g.L}^{-1}$ in POM). The insignificant variation between PRM and POM indicates the consistency of a similar source of origin (geological crustal) during both seasonal periods (Mondal et al., 2010; Bhutiani et al., 2016; Singh and Kamal 2017). The concentration of Fe in approximately 49% of samples in PRM and POM was above the permissible limit of $300 \mu\text{g.L}^{-1}$ given by (BIS, 2012). Mn, another abundant crustal element usually found in groundwater (Singh and Kamal, 2017), revealed concentrations of GM: $145.57 \pm 170.79 \mu\text{g.L}^{-1}$ in PRM and GM: $178.07 \pm 338.07 \mu\text{g.L}^{-1}$ in POM. Mn in 37% and 42% of the PRM and POM samples, respectively, found exceeding the permissible limit of $100 \mu\text{g.L}^{-1}$ (BIS, 2012).

Arsenic (As) has been categorized as a human carcinogen that results

in skin and lung cancer (IARC, 2012). Exposure at higher levels can cause severe neurological, cardiovascular, reproductive, and respiratory disorders (Wang et al., 2007; Rahman et al., 2009). The concentration of As in groundwater was found GM: $7.22 \pm 3.46 \mu\text{g.L}^{-1}$ and GM: $7.29 \pm 2.57 \mu\text{g.L}^{-1}$ in PRM and POM, respectively, with a higher concentration in 11% PRM and 24% POM samples compared to the permissible level of $10 \mu\text{g.L}^{-1}$ (WHO, 2011). The higher concentration of Fe and Mn oxides and As suggests that it is mobilized because of the reductive dissolution of Fe and Mn oxides with As-oxy anions in groundwater aquifer (Rahman et al., 2009).

Aluminium was found to be GM: $8.01 \pm 21.60 \mu\text{g.L}^{-1}$ (PRM) and GM: $5.82 \pm 18.05 \mu\text{g.L}^{-1}$ (POM) in groundwater samples with exceeding in

Table 2

Varimax orthogonal rotation factor loadings of twenty-seven parameters of groundwater on execution of PCA for PRM and POM periods.

Parameters	Components					
	Pre monsoon			Post monsoon		
	Factor 1	Factor 2	Factor 3	Factor 1	Factor 2	Factor 3
Li	0.879	0.078	0.095	0.929	0.123	0.007
Be	0.867	0.101	0.078	0.904	0.011	0.048
B	0.025	0.213	0.924	-0.017	0.153	0.921
Al	0.128	0.220	0.903	0.020	0.255	0.878
V	0.936	0.011	0.064	0.915	0.181	0.006
Cr	0.862	-0.069	-0.014	0.965	0.094	0.020
Mn	-0.101	0.781	0.249	0.167	0.884	0.025
Fe	0.068	0.837	0.281	0.272	0.789	-0.041
Se	0.847	-0.088	0.19	0.873	0.081	-0.057
Co	0.204	0.655	0.201	0.007	0.811	0.043
Ni	0.948	0.003	0.021	0.819	0.039	0.029
Cu	0.940	0.071	0.111	0.917	0.159	0.125
Zn	-0.013	0.127	0.906	0.129	0.169	0.839
As	0.093	0.771	-0.033	0.060	0.789	0.054
Cd	0.945	0.022	0.026	0.936	0.128	0.011
Sn	0.908	0.005	0.055	0.958	0.040	0.052
Sb	0.869	-0.048	-0.054	0.942	0.115	0.001
Ba	-0.210	0.816	-0.034	0.051	0.780	0.112
Mg ²⁺	0.131	0.921	0.177	0.125	0.897	0.245
Na ⁺	0.873	0.097	0.117	0.847	0.005	0.064
K ⁺	0.910	0.040	0.083	0.921	0.098	0.137
Ca ²⁺	0.113	0.902	0.166	-0.094	0.799	0.271
Cl ⁻	0.161	0.191	0.903	0.303	-0.148	0.427
F ⁻	-0.110	0.870	0.127	0.007	0.718	-0.160
NO ₃ ⁻	0.061	0.195	0.933	0.124	0.165	0.919
SO ₄ ²⁻	0.829	0.199	0.216	0.938	0.154	0.022
HCO ₃ ⁻	0.553	0.721	-0.027	0.210	0.862	0.052

Table 3

Factor values of different parameters used for calculation of exposure assessment.

Parameter	Value		Reference
	Children	Adult	
IR	1Lday ⁻¹	2 L day ⁻¹	EPA (1989)
EF	365 days year ⁻¹	365 days year ⁻¹	USEPA (2004)
ED	12 years	30 years	USEPA (2004)
CF	10 ⁻³	10 ⁻³	Yavar Ashayeri and Keshavarzi (2019)
BW	15 kg	70 kg	USEPA (2004)
AT	ED × 365 day (non-carcinogen)	70 × 365 = 25,550 days (carcinogen)	USEPA (2004) (Islam et al., 2019)
SA	18000 cm ²	6600 cm ²	(USEPA, 2011)
Kp	Ba = 0.07, Be = 0.007, Cd = 0.05, Cr = 0.025, Ni = 0.04, Sb = 0.15, V = 0.026, for other elements = 1		(US-EPA, 2014) Hu et al. (2012)

11% and 6% samples in PRM and POM samples from the permissible limit of 30 µg.L⁻¹ (BIS, 2012). Higher Al concentrations may disturb the physical and cellular process of the body as it replaces the Mg²⁺ and Fe³⁺ ions in the body disrupting the cellular function, secretory function, and intercellular interactions (Ravindra and Mor, 2019). Ni, a potentially toxic element, was also found exceeding the permissible limits of 20 µg.L⁻¹ in 16% and 9% samples of PRM and POM, respectively (BIS, 2012). Sites with higher groundwater Ni concentrations are mostly located in agricultural fields. The use of Ni-enriched insecticides/fertilizers might be the primary reason for increased Ni concentration in groundwater samples (Gimeno-García et al., 1996; Defarge et al., 2018). Other measured elemental species (B, Ba, Be, Cd, Cr, Co, Cu, Li, Se, Sn, Sb, V, Zn) were found in trace amounts and within the respective permissible limits for drinking water.

4.2. Spatiotemporal variability of trace elements

The coefficient of spatial variation (CV), determined by dividing the standard deviation by the overall mean across the sites, is presented in Table 1 separately for DW and BW sites and for PRM and POM seasons to

evaluate spatiotemporal variability. A graph was also plotted using origin 8.1 between the values obtained by dividing %CV for each trace element in POM by PRM and visa-versa with a mathematical factor >1 to evaluate spatiotemporal variability (Fig. 2). Except for Fe, As, Co, and Mn, all other elemental species concentrations have shown higher spatial variability of >100% across both DW and BW sites during PRM. It underscores the wide contribution of mineral-rich beds to hydro-chemistry of the study region through mineral dissolution. On evaluating the spatial variability in temporal scale (spatiotemporal variability) across DW sites, Cu, Zn, Ni, Mn, Al and B elemental concentrations have shown multi-fold higher spatial variability in PRM compared to the POM period. On the contrary, CV% associated with Co, Sb, and Cr concentrations were higher in POM than PRM. In BW sites, concentrations of several elements (As, Zn, Ni, Co, Mn, Cr, V) have shown higher spatial variability in PRM than POM. This may be attributed to an increase in mineral concentration and a decrease in groundwater table during PRM.

4.3. Factor analysis using PCA technique

The principal component analysis (PCA) is a receptor technique for recognizing patterns, explaining the variance of significant inter-correlated variables, and could be altered to independent variables (Helena et al., 2000; Krishna et al., 2009; Belkhiri and Narany 2015). PCA method has been described in detail in S1. PCA was executed for extracting significant factors to evaluate possible source types of groundwater chemical contaminants using chemical profiles of elemental concentrations along with reported ionic concentrations.

Factors were determined with a group of heavy elements and ions in groundwater which were strongly correlated in the factor matrix after operating the varimax rotation (Table 2). Supplementary Tables S2–S3 show details of PCA including principal components (PCs), percentage of variance, and cumulative percentage of each PCs for PRM and POM period respectively. KMO and Bartlett's sphericity test was performed in data sets of both PRM and POM periods for examining the accuracy of factor analysis and found $p = 0.85$ (for PRM) and $p = 0.84$ (for POM), well beyond the prescribed values of $p > 0.5$ (Haji Gholizadeh et al., 2016). Similarly, χ^2 -values were also within prescribed good fit parameters, underscore the appropriateness of factor analysis using PCA.

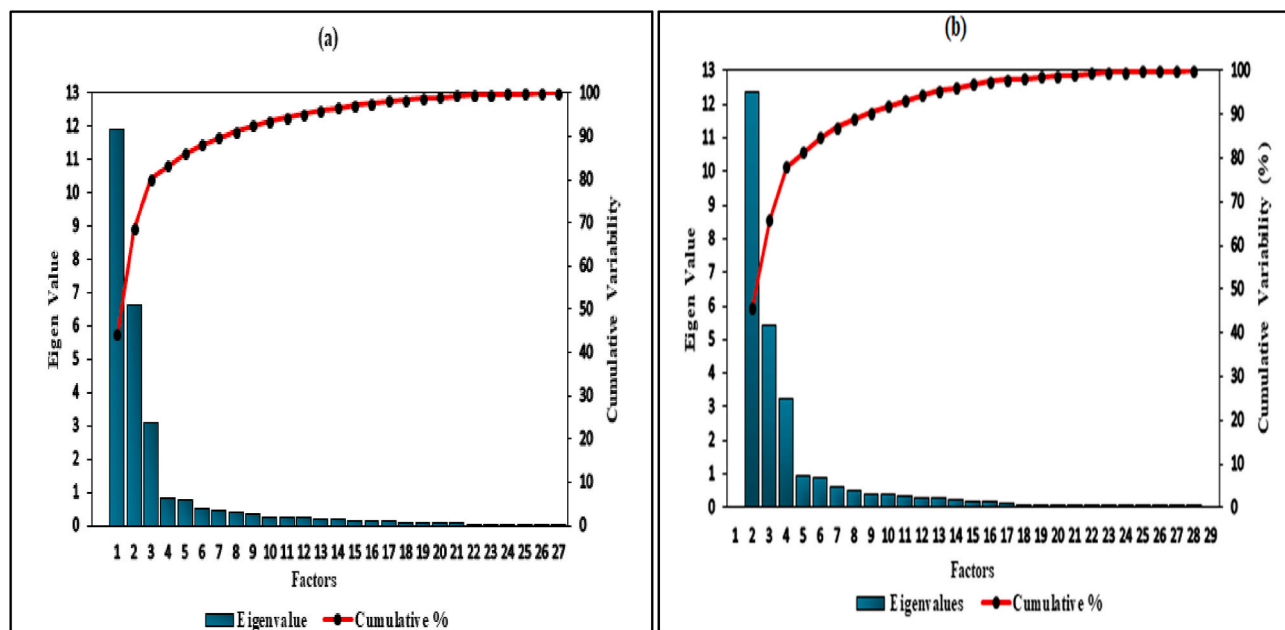


Fig. 3. Scree plot drawn for determining the number of factors in PCA receptor model indicating common source of chemical species in groundwater during (a) PRM and (b) POM periods.

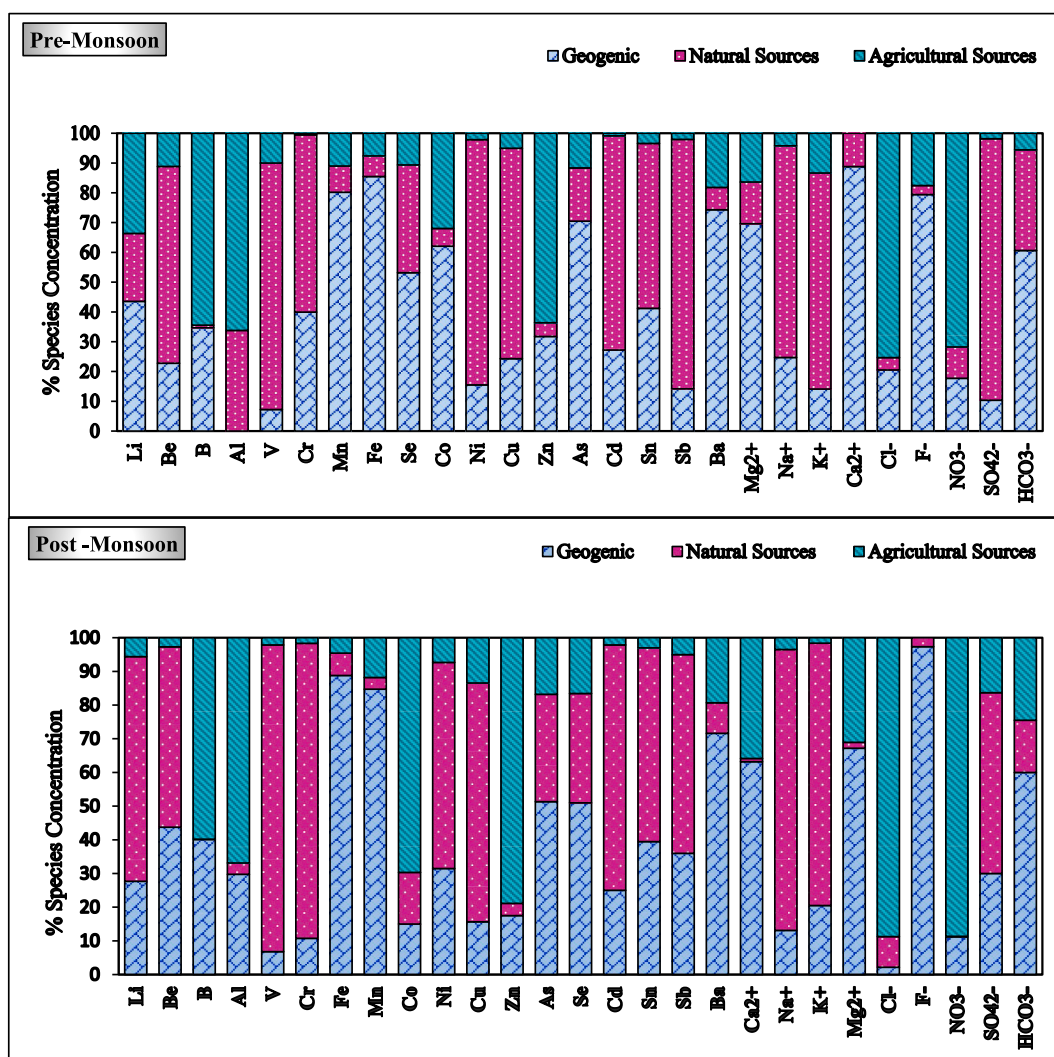


Fig. 4. The relative contribution estimates of source-factors of trace and potentially toxic elements using EPA PMF 5.0 model for pre-monsoon and post-monsoon periods.

The total variance was found 80.18% (PRM) and 77.95% (POM). Three factors were extracted by relevant variables based on Kaiser's rule as the Eigenvalue for the first three components was >1 in both sampling periods. The scree plots of PRM and POM were depicted in Fig. 3(a) and (b). The first factor exhibits 42.53% (PRM) and 43.68% (POM) of total variance with a positive factor loading of Be, Cd, Cr, Cu, K⁺, Li, Na⁺, Ni, Se, Sb, Sn, V, and SO₄²⁻ while negative loading on Ba, F⁻ and Mn. Interaction of acidic components of atmospheric wet precipitation with soil, followed by percolation to groundwater might be the indicator of the first source factor. This factor could be attributed to the natural sources which signify the percolation of elements and ions present in the soil through the rainwater or may enter the groundwater aquifer through surface water via various biochemical processes such as oxidation-reduction and ion exchange etc. (Drever 1997; Sethy et al., 2016; Loh et al., 2020).

The second factor shows 20.84% (PRM) and 19.19% (POM) of total variance with a positive factor loading of As, Ba, Ca²⁺, Co, F⁻, Fe, HCO₃⁻, Mg²⁺, and Mn while negative loading of Cr, Se, and Sb. The second factor might be originated by geogenic sources, which resulted in the dissolution of minerals like calcite [CaCO₃] and iron oxides (e.g. goethite [FeO(OH)] and hematite [Fe₂O₃]) (Lu et al., 2012; Kashyap et al., 2018). Crustal elements, e.g. Fe, Mn, Ca²⁺, and Mg²⁺ found in minerals present in the study area are dissolved into groundwaters by rock-water interaction processes.

The third factor exhibits 16.82% (PRM) and 15.07% (POM) of total variance with a positive factor loading of Al, B, Cl⁻, NO₃⁻ and Zn while negative factor loading of Cr, As, Sb, Ba, and HCO₃⁻. This factor could be attributed to the agricultural sources as the fertilizer-rich water may enter the aquifer and contaminate the groundwater (Hudak 2012; Jassas and Merkel 2015).

4.4. Source apportionment using positive matrix factorization (PMF 5.0)

U.S. EPA's PMF 5.0 was executed using chemical profiles of 27 chemical species (concentrations and related uncertainties) of 160 groundwater samples for source apportionment of ions and heavy elements during PRM and POM sampling seasons, respectively. PMF 5.0 receptor model has been described in detail in S2. The Optimal number of factors (03) were determined by the iteration with the lowest Q (Robust)/Qexp value, picked up by performing 20 random runs (Paatero 1997; Norris et al., 2014). The factor fingerprints, obtained from PMF5.0, were presented using the percentage of individual species concerning all species and the species concentration related to source factors have been shown in Fig. 4. Species with >50% contribution were used to designate a particulate source-factor. The factor profile of groundwater chemical species for PRM and POM has been shown in Figs. 5 and 6 respectively.

In PRM, Factor 1 contributes 41.26% to chemical contaminants of

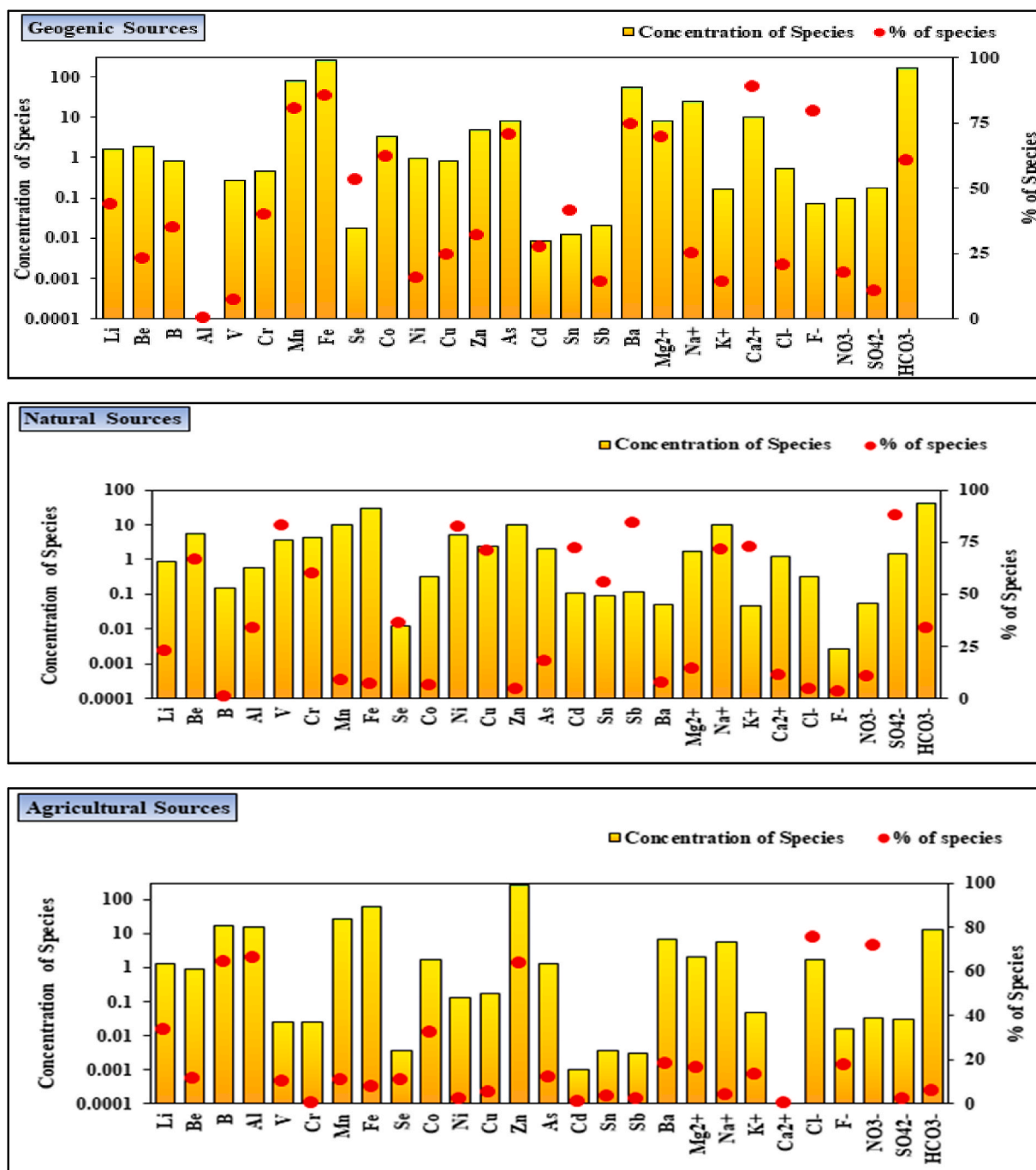


Fig. 5. Factor profile of chemical species in groundwater determined using EPA PMF5.0 receptor model for pre-monsoon period.

groundwater samples with a major contribution of Mn, Fe, Se, Co, Ba, F^- , Ca^{2+} , As, Mg^{2+} , Ba, and HCO_3^- species derived from geogenic sources viz. rock weathering (e.g. fluorite [CaF_2], hematite and arsenopyrite [$FeAsS$]) into groundwaters (Lu et al., 2012; Mahato et al., 2016). Factor 2 is characterized by higher concentrations of Be, V, Cr, Ni, Cu, Cd, Sn, Sb, Na^+ , K^+ and SO_4^{2-} with 35.97% factor contribution, indicates the natural source. These chemical species are commonly found in soil and may enter the groundwater aquifers by percolation through rainwater or surface water (Chen et al., 2019; Loh et al., 2020).

Factor 3 represents the agricultural sources with a 20.76% factor contribution and higher factor loading of B, Al, Zn, Cl^- and NO_3^- (Jassas and Merkel, 2015). Comparatively higher contribution of geogenic sources in PRM might be due to lowering in groundwater table in summertime (PRM), consequently increasing the concentrations of

species known for geogenic origin.

For the POM period, Factor 1 has shown 38.56% factor contribution with a higher concentration of V, Cr, Ni, Cu, Cd, Se, Sn, Sb, Na^+ , K^+ , and SO_4^{2-} ; representing the natural sources. Factor 2 contributes 36.56% with a higher factor loading of Fe, Mn, As, Se, Ba, Ca^{2+} , Mg^{2+} , F^- , HCO_3^- , representing the geogenic sources. In contrast, Factor 3 has shown 25.10% factor contribution, representing the agricultural sources with a higher concentration of B, Al, Co, Zn, Cl^- and NO_3^- . The relatively higher contribution of natural sources in groundwater contamination in the POM period might be due to wet monsoon precipitation. The average contribution of sources in PRM and POM is shown in Fig. 7

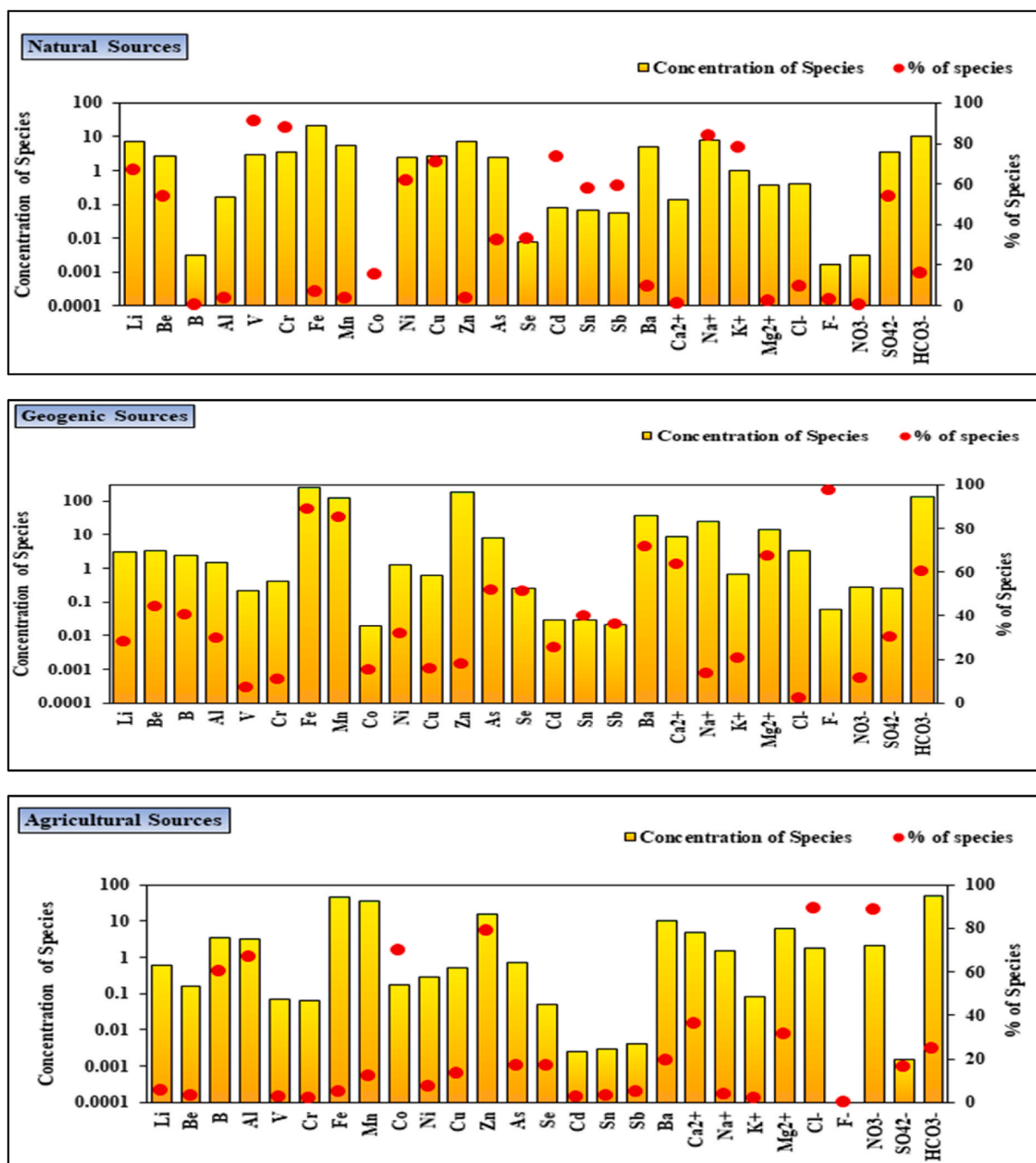


Fig. 6. Factor profile of chemical species in groundwater determined using EPA PMF5.0 receptor model for post-monsoon period.

4.5. Inter-comparison of PCA and PMF results

Source identifications and quantitative source contribution estimates of groundwater chemical contaminants were performed using the PCA and PMF 5.0 receptor modelling techniques, respectively. Both methods are different in the aspects of the software, method, and associated operations. In PCA, scree plot and KMO values were used to estimate the principal components or number of factors. Whereas in PMF 5.0, factor fingerprint represented the factor contribution of each chemical species, which was used to identify the marker species for each factor. Although both models have shown a similar source of the chemical contaminant of groundwater samples. But PCA technique is limited to predicting the possible source factors, whereas PMF5.0 results are quantitative and more precise as it is applicable in complete data including outliers and

can estimate each source's composition (Comero et al., 1999).

4.6. Health risk assessment

Health risk assessment is an important aspect to understand the potential of trace elements to cause health hazards in humans via different exposure routes. Health risk has been evaluated for the heavy elements in groundwater samples through oral and dermal exposure routes in children and adults. For evaluating the annual health risk data, the mean value of PRM and POM concentrations has been considered. Outcomes of health risk analysis relevant to the carcinogenic and non-carcinogenic risks have been summarized in Table 4.

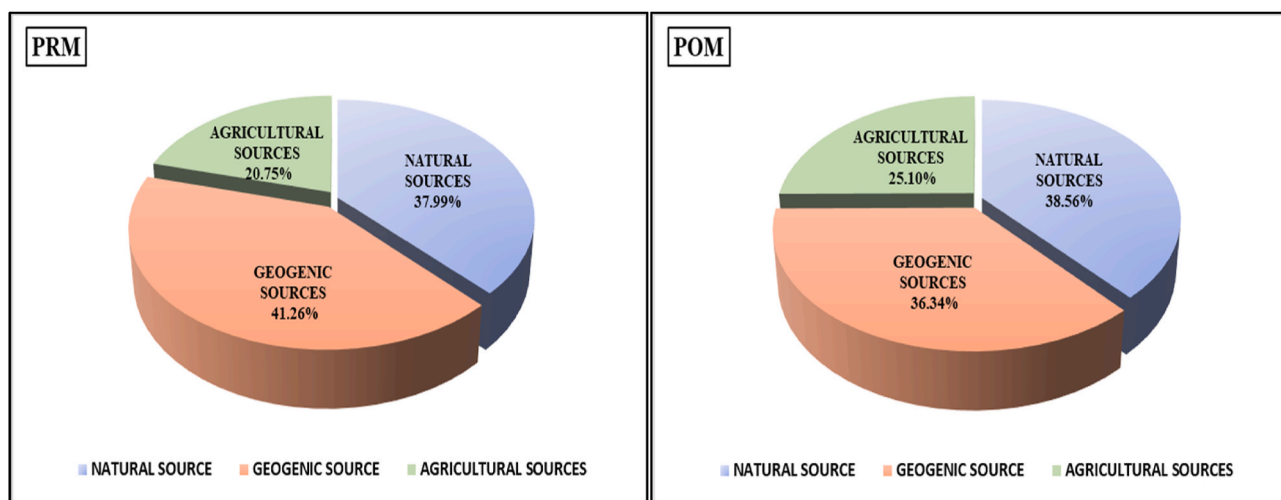


Fig. 7. Estimation of average contributions of sources in PRM and POM using EPA PMF 5.0 model.

Table 4

Average daily dose of each element from different exposure pathways: HQ, hazard quotient; HI, hazard index of groundwater; CR, Carcinogenic Risk.

Non-Carcinogenic Risk										
Species	CDI (mg.kg ⁻¹ . day ⁻¹)		DAD (mg.kg ⁻¹ . day ⁻¹)		HQ _{ing}		HQ _d		HI	
	Children	Adult	Children	Adult	Children	Adult	Children	Adult	Children	Adult
Al	4.62E-04	1.98E-04	1.22E-06	7.12E-07	4.62E-04	1.98E-04	1.22E-06	7.12E-07	4.63E-04	1.99E-04
As	4.84E-04	2.07E-04	1.28E-06	7.46E-07	1.61 E+00	6.91E-01	4.26E-03	2.49E-03	1.62 E+00	6.94E-01
Ba	4.70E-03	2.01E-03	1.24E-05	7.25E-06	2.35E-02	1.01E-02	8.86E-04	5.18E-04	2.44E-02	1.06E-02
Be	4.10E-04	1.76E-04	1.08E-06	6.32E-07	2.05E-01	8.78E-02	7.72E-02	4.51E-02	2.82E-01	1.33E-01
B	6.78E-04	2.90E-04	1.79E-06	1.05E-06	3.39E-03	1.45E-03	8.95E-06	5.23E-06	3.40E-03	1.46E-03
Cd	7.52E-04	3.22E-04	1.99E-06	1.16E-06	7.52E-01	3.22E-01	3.97E-02	2.32E-02	7.92E-01	3.46E-01
Co	5.80E-05	2.49E-05	1.53E-07	8.95E-08	1.93E-01	8.28E-02	5.10E-04	2.98E-04	1.94E-01	8.31E-02
Cr	9.56E-05	4.10E-05	2.52E-07	1.47E-07	3.19E-02	1.37E-02	3.36E-03	1.97E-03	3.52E-02	1.56E-02
Cu	1.41E-04	6.06E-05	3.73E-07	2.18E-07	3.53E-03	1.51E-03	9.33E-06	5.45E-06	3.54E-03	1.52E-03
Fe	2.49E-02	1.07E-02	6.56E-05	3.84E-05	3.55E-02	1.52E-02	9.38E-05	5.48E-05	3.56E-02	1.53E-02
Li	4.24E-04	1.82E-04	1.12E-06	6.55E-07	2.12E-01	9.09E-02	5.60E-04	3.27E-04	2.13E-01	9.13E-02
Mn	1.08E-02	4.62E-03	2.85E-05	1.66E-05	7.71E-02	3.30E-02	2.03E-04	1.19E-04	7.73E-02	3.31E-02
Ni	2.16E-04	9.25E-05	5.70E-07	3.33E-07	1.08E-02	4.62E-03	7.12E-04	4.16E-04	1.15E-02	5.04E-03
Sb	3.79E-06	1.62E-06	1.00E-08	5.84E-09	9.47E-03	4.06E-03	1.67E-04	9.74E-05	9.64E-03	4.16E-03
Se	9.30E-06	3.99E-06	2.46E-08	1.44E-08	1.86E-03	7.97E-04	4.91E-06	2.87E-06	1.87E-03	8.00E-04
V	4.60E-05	1.97E-05	1.22E-07	7.10E-08	9.21E-03	3.95E-03	9.35E-04	5.46E-04	1.01E-02	4.49E-03
Zn	1.45E-02	6.22E-03	3.83E-05	2.24E-05	4.83E-02	2.07E-02	1.28E-04	7.46E-05	4.85E-02	2.08E-02
F ⁻	1.02E-02	4.38E-03	2.70E-05	1.58E-05	2.56E-01	1.10E-01	6.75E-04	3.94E-04	2.56E-01	1.10E-01
NO ₃ ⁻	1.36E-01	5.82E-02	3.58E-04	3.84E-05	8.49E-02	3.64E-02	2.24E-04	2.40E-05	8.51E-02	3.64E-02
Sum	2.05E-01	8.77E-02	5.40E-04	1.45E-04	3.57E + 00	1.53E + 00	1.30E-01	7.57E-02	3.70E + 00	1.61E + 00
Carcinogenic Risk										
Species	CDI (mg.kg ⁻¹ . day ⁻¹)		DAD (mg.kg ⁻¹ . day ⁻¹)		CR _{ing}		CR _d		CR	
	Children	Adult	Children	Adult	Children	Adult	Children	Adult	Children	Adult
As	4.84E-04	2.07E-04	1.28E-06	7.46E-07	7.26E-04	3.11E-04	1.92E-06	1.12E-06	7.28E-04	3.12E-04
Cr	9.56E-05	4.10E-05	2.52E-07	1.47E-07	4.78E-05	2.05E-05	5.05E-06	2.95E-06	5.28E-05	2.34E-05
Sum	5.79E-04	2.48E-04	1.53E-06	8.94E-07	7.73E-04	3.31E-04	6.96E-06	4.07E-06	7.80E-04	3.36E-04

4.6.1. Non-carcinogenic risk assessment

To compute the extent of health hazard resulted due to the exposure to trace and potentially toxic heavy metals/metalloids (n = 19), hazard quotient (HQ) and hazard index (HI) were evaluated. Reference Dose (RfD) values were available only for Al, As, Ba, Be, B, Cd, Co, Cr, Cu, Fe, Li, Mn, Ni, Sb, Se, V, Zn, F⁻, and NO₃⁻. Therefore, the non-carcinogenic risk was evaluated only for these elements. The computed overall non-carcinogenic ingestion risk (HQ_{ing}) values for children was (3.57 E+00) while for adults (1.53 E+00). The lowest and the highest non-carcinogenic risk associated with exposure via ingestion was estimated for Al and As. It is noteworthy that HQ_{ing} for all the elements was <1.00 E+00, except for As in children. The HQ_{ing} values of As for children was

(1.61 E+00), which indicates that children are more susceptible to the non-carcinogenic risk posed by drinking As contaminated water. Higher ingestion of As may have a negative impact on the growth of children and may trigger cardiovascular diseases (WHO, 2011). The total non-carcinogenic dermal risk (HQ_d) value for adults and children was 1.30E-01 and 7.57E-02, respectively, within the safe limit of HQ_d = 1.00 E+00 for all the elements. It indicates non-carcinogenic dermal risk in adults as well as in children.

Non-carcinogenic total risk estimated by HI_{total} value evaluated for both the exposure routes both in children and adults was found 3.70 E+00 and 1.61 E+00, respectively, above the threshold limit of 1.00 E+00. The HI value of all other elements was within the limit except for

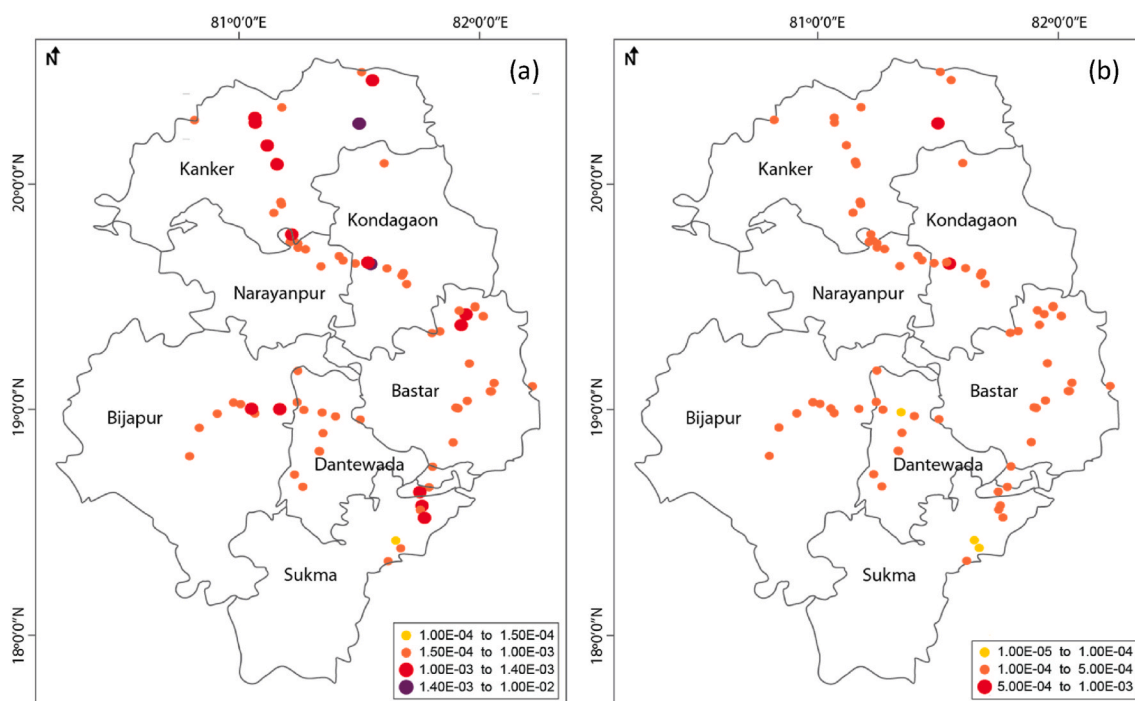


Fig. 8. Total Risk distribution for (a) children; and (b) adults.

As ($1.62 \text{ E}+00$) in children. The results show that the non-carcinogenic risk is posed only by the As in the groundwater of the study area and children are more susceptible to risk than adults.

4.6.2. Carcinogenic risk assessment

The potential carcinogenic risk was estimated for only As and Cr as the slope factor was available only for these two elements. The overall carcinogenic risk calculated via the ingestion route (CR_{ing}) was $7.73\text{E}-04$ in children and $3.31\text{E}-04$ in adults, both above the maximum threshold limit ($1.00\text{E}-04$). The results estimated for groundwater of the study area have shown that among the two elements, As has a higher CR the ingestion risk is $7.76\text{E}-04$ and $3.11\text{E}-04$ for children and adults, respectively. It suggests that lifelong consumption of As-rich water may raise the cancer risk in the inhabitants. The total carcinogenic dermal risk (CR_d) in children and adults was below the safe limit ($1.00\text{E}-04$). The total carcinogenic risk (CR) from As and Cr in children and adult groups were found to be $7.80\text{E}-04$ and $3.36\text{E}-04$, respectively.

While As resulted in CR value of $7.28\text{E}-04$ in children and $3.12\text{E}-04$ in adults. The results suggested that the carcinogenic risk is more vulnerable to children than to adults. CR distribution by samples on the study area is presented in Fig. 8. The CR distribution shows that the geogenic sources (mineral leaching) may be the major contributor of arsenic in the groundwater of the study region. Volcanic rock weathering leads to the leaching of arsenic onto ferric hydroxide and gets deposited with the sediment which later on interaction with groundwater aquifers result in As contamination of groundwater (Pandey et al., 2006).

5. Conclusion

This study reports the spatiotemporal variability, source apportionment, and health risk assessment of trace and toxic elements, including heavy metals, ions, and metalloids in the groundwater of the tribal belt of the Bastar region. The concentration of Al, As, Fe, Mn, and Ni were significantly higher than the permissible limit in the groundwater of the study area in both PRM and POM. Source apportionment result of PCA and PMF shows that Natural, geogenic, and agricultural sources contributed to the groundwater chemical contaminants in the study

area.

The exposure risk model has shown that all elements were under a safe limit except for As, which has shown higher carcinogenic and non-carcinogenic risk values. Result predicts that prolonged exposure to arsenic through contaminated water may cause carcinogenic or non-carcinogenic risks among the inhabitants of the study area. It is noteworthy that children were more susceptible to the carcinogenic and non-carcinogenic risk as compared to adults. Hence, a conclusion can be drawn that the overall groundwater of the field area is appropriate for both drinking except for some locations where concentrations of some trace elements, especially As are higher and require proper groundwater treatment. Very few works have been done in the Bastar region on groundwater quality. Thus, this study would provide detailed knowledge so that policymakers would take proper steps to improve the water quality of the Bastar region. Further awareness among the people regarding the harmful health impacts resulting from toxic elements in groundwater is desired.

Declaration of competing interest

The authors declare the following financial interests/personal relationships which may be considered as potential competing interests: Shamsh Pervez reports financial support was provided by Science and Engineering Research Board. Princy Dugga reports financial support was provided by University Grants Commission.

Acknowledgment

The presented piece of work was primarily supported by the Science and Engineering Research Board (SERB), India (EMR/2015/000928) and partially supported by the DST FIST program (SR/FST/CSI-259/2014 (c)) and UGC-SAP-DRS-II program (F-540/7/DRS-II/2016 (SAP-I)). Princy Dugga (PD) is grateful to UGC and Pt. Ravishankar Shukla University for providing Joint UGC-CSIR Fellowship [F.No.16-6 (Dec.2017)/2018(NET/CSIR)] along with laboratory and library facilities, respectively. Authors Shamsh Pervez (SP) and (PD) are also grateful to Thermo Fischer Scientific, Mumbai (India) for providing instrumentation facilities.

Appendix A. Supplementary data

Supplementary data to this article can be found online at <https://doi.org/10.1016/j.gsd.2021.100628>.

References

- Ahada, C.P.S., Suthar, S., 2018. Assessing groundwater hydrochemistry of Malwa Punjab, India. *Arab. J. Geosci.* 11 <https://doi.org/10.1007/s12517-017-3355-8>.
- Behera, B., Das, M., Rana, G.S., 2012. Studies on ground water pollution due to iron content and water quality in and around, Jagdalpur, Bastar district, Chattisgarh, India. *J. Chem. Pharmaceut. Res.* 4, 3803–3807.
- Belkhir, L., Narany, T.S., 2015. Using multivariate statistical analysis, geostatistical techniques and structural equation modeling to identify spatial variability of groundwater quality. *Water Resour. Manag.* 29, 2073–2089.
- Bhuti, R., Kulkarni, D.B., Khanna, D.R., Gautam, A., 2016. Water quality, pollution source apportionment and health risk assessment of heavy metals in groundwater of an industrial area in North India. *Expo. Heal* 8, 3–18. <https://doi.org/10.1007/s12403-015-0178-2>.
- BIS, 2012. Indian standard drinking water specification (second revision). *Bur. Indian Stand. IS 10500*, 1–11.
- Boateng, T.K., Opoku, F., Acquah, S.O., Akoto, O., 2016. Groundwater quality assessment using statistical approach and water quality index in Ejisu-Juaben Municipality, Ghana. *Environ. Earth Sci.* 75, 1–14. <https://doi.org/10.1007/s12665-015-5105-0>.
- Bouderbala, A., Gharbi, B.Y., 2017. Hydrogeochemical characterization and groundwater quality assessment in the intensive agricultural zone of the Upper Chelif plain, Algeria. *Environ. Earth Sci.* 76, 1–17. <https://doi.org/10.1007/s12665-017-7067-x>.
- Brindha, K., Paul, R., Walter, J., Tan, M.L., Singh, M.K., 2020. Trace metals contamination in groundwater and implications on human health: comprehensive assessment using hydrogeochemical and geostatistical methods. *Environ. Geochem. Health* 42, 3819–3839. <https://doi.org/10.1007/s10653-020-00637-9>.
- Chen, R., Teng, Y., Chen, H., Hu, B., Yue, W., 2019. Groundwater pollution and risk assessment based on source apportionment in a typical cold agricultural region in Northeastern China. *Sci. Total Environ.* 696, 133972. <https://doi.org/10.1016/j.scitotenv.2019.133972>.
- Clark, R., Lawrence, A., Foster, S., 1996. *Groundwater: A Threatened Resource*. United Nations Environ. Program.
- Comero, S., Capitani, L., Gawlik, B.M., 1999. Positive Matrix Factorisation (PMF) Environmental Monitoring Data Using PMF. *Environmetrics*. <https://doi.org/10.2788/2497>.
- Defarge, N., Spiroux de Vendômois, J., Séralini, G.E., 2018. Toxicity of formulations and heavy metals in glyphosate-based herbicides and other pesticides. *Toxicol. Rep.* 5, 156–163. <https://doi.org/10.1016/j.toxrep.2017.12.025>.
- <https://doh.gov.in/sites/default/files/Default/ContentColl/CG%20opt.pdf>.
- Dora, M.L., 2014. PGE mineralization in Bastar Craton, central India: prospects and constraints. *Indian J. Geosci.* 68.
- Drever, J.I., 1997. *The Geochemistry of Natural Waters: Surface and Groundwater Environments*, third ed. Prentice Hall, Upper Saddle River, NJ).
- Dugga, P., Pervez, S., Tripathi, M., Siddiqui, M.N., 2020. Spatiotemporal variability and source apportionment of the ionic components of groundwater of a mineral-rich tribal belt in Bastar, India. *Groundw. Sustain. Dev.* 10 <https://doi.org/10.1016/j.gsd.2020.100356>.
- Duggal, V., Rani, A., 2018. Carcinogenic and Non-carcinogenic Risk Assessment of Metals in Groundwater via Ingestion and Dermal Absorption Pathways for Children and Adults in Malwa Region of Punjab, vol. 92, pp. 187–194. <https://doi.org/10.1007/s12594-018-0980-0>.
- Edition, F., 2011. *Guidelines for drinking-water quality*. *WHO Chron.* 38, 104–108.
- El Nemr, A., El-Said, G.F., Ragab, S., Khaled, A., El-Sikaily, A., 2016. The distribution, contamination and risk assessment of heavy metals in sediment and shellfish from the Red Sea coast, Egypt. *Chemosphere* 165, 369–380. <https://doi.org/10.1016/j.chemosphere.2016.09.048>.
- Emenike, P.G.C., Tenebe, I., Ogareke, N., Omole, D., Nnaji, C., 2019. Probabilistic risk assessment and spatial distribution of potentially toxic elements in groundwater sources in Southwestern Nigeria. *Sci. Rep.* 9, 1–15. <https://doi.org/10.1038/s41598-019-52325-z>.
- EPA, 1989. *Risk Assessment Guidance for Superfund. Volume I Human Health Evaluation Manual (Part A) I*, p. 289.
- Gimeno-García, E., Andreu, V., Boluda, R., 1996. Heavy metals incidence in the application of inorganic fertilizers and pesticides to rice farming soils. *Environ. Pollut.* 92, 19–25. [https://doi.org/10.1016/0269-7491\(95\)00090-9](https://doi.org/10.1016/0269-7491(95)00090-9).
- Guo, X., Zuo, R., Shan, D., Cao, Y., Wang, J., Teng, Y., Fu, Q., Zheng, B., 2017. Source apportionment of pollution in groundwater source area using factor analysis and positive matrix factorization methods. *Hum. Ecol. Risk Assess.* 23, 1417–1436. <https://doi.org/10.1080/10807039.2017.1322894>.
- Gupta, A., Kumar, S., Shekhar, S., J, A.M.-I.I., 2016. undefined, 2012. *Water and Food Security of the Central Indian Craton*. Academia, Edu.
- Haji Gholizadeh, M., Melesse, A.M., Reddi, L., 2016. Water quality assessment and apportionment of pollution sources using APCS-MLR and PMF receptor modeling techniques in three major rivers of South Florida. *Sci. Total Environ.* 566 (567), 1552–1567. <https://doi.org/10.1016/j.scitotenv.2016.06.046>.
- Helena, B., Pardo, R., Vega, M., Barrado, E., Fernandez, J.M., Fernandez, L., 2000. Temporal evolution of groundwater composition in an alluvial aquifer (Pisuerga River, Spain) by principal component analysis. *Water Res.* 34, 807–816.
- Hossain, M., Patra, P.K., 2020. Contamination zoning and health risk assessment of trace elements in groundwater through geostatistical modelling. *Ecotoxicol. Environ. Saf.* 189, 110038. <https://doi.org/10.1016/j.ecoenv.2019.110038>.
- Hu, G., Mian, H.R., Dyck, R., Mohseni, M., Jasim, S., Hewage, K., Sadiq, R., 2020. Drinking water treatments for arsenic and manganese removal and health risk assessment in white rock, Canada. *Expo. Heal* 12, 793–807. <https://doi.org/10.1007/s12403-019-00338-4>.
- Hudak, P.F., 2012. Nitrate and chloride concentrations in groundwater beneath a portion of the trinity group outcrop zone, Texas. *Int. J. Environ. Res.* 6, 663–668. <https://doi.org/10.22059/ijer.2012.536>.
- IARC Working Group on the Evaluation of Carcinogenic Risks to Humans, 2012. *Chemical agents and related occupations*. IARC Monogr. Eval. Carcinog. Risks Hum. 100, 9–562.
- Islam, A.R.M.T., Bodrud-Doza, M., Rahman, M.S., Amin, S.B., Chu, R., Al Mamun, H., 2019. Sources of Trace Elements Identification in Drinking Water of Rangpur District, Bangladesh and Their Potential Health Risk Following Multivariate Techniques and Monte-Carlo Simulation, Groundwater for Sustainable Development. Elsevier B.V. <https://doi.org/10.1016/j.gsd.2019.100275>.
- Jassas, H., Merkel, B., 2015. Assessment of hydrochemical evolution of groundwater and its suitability for drinking and irrigation purposes in Al-Khazir Gomal Basin, Northern Iraq. *Environ. Earth Sci.* 74, 6647–6663. <https://doi.org/10.1007/s12665-015-4664-4>.
- Kashyap, R., Verma, K.S., Uniyal, S.K., Bhardwaj, S.K., 2018. Geospatial distribution of metal(loid)s and human health risk assessment due to intake of contaminated groundwater around an industrial hub of northern India. *Environ. Monit. Assess.* 190 <https://doi.org/10.1007/s10661-018-6525-6>.
- Krishna, A.K., Satyanarayanan, M., Govil, P.K., 2009. Assessment of heavy metal pollution in water using multivariate statistical techniques in an industrial area: a case study from Patancheru, Medak District, Andhra Pradesh, India. *J. Hazard Mater.* 167, 366–373. <https://doi.org/10.1016/j.jhazmat.2008.12.131>.
- Li, P., Li, X., Meng, X., Li, M., Zhang, Y., 2016. Appraising groundwater quality and health risks from contamination in a semiarid region of Northwest China. *Expo. Heal* 8, 361–379. <https://doi.org/10.1007/s12403-016-0205-y>.
- Liu, J., Gao, M., Jin, D., Wang, T., Yang, J., 2020. Assessment of groundwater quality and human health risk in the aeolian-sand area of Yulin City, Northwest China. *Expo. Heal* 12, 671–680. <https://doi.org/10.1007/s12403-019-00326-8>.
- Loh, Y.S.A., Akurugu, B.A., Manu, E., Aliou, A.S., 2020. Assessment of groundwater quality and the main controls on its hydrochemistry in some Voltaian and basement aquifers, northern Ghana. *Groundw. Sustain. Dev.* 10, 100296. <https://doi.org/10.1016/j.gsd.2019.100296>.
- Lu, K.L., Liu, C.W., Jang, C.S., 2012. Using multivariate statistical methods to assess the groundwater quality in an arsenic-contaminated area of Southwestern Taiwan. *Environ. Monit. Assess.* 184, 6071–6085. <https://doi.org/10.1007/s10661-011-2406-y>.
- Mahato, M.K., Singh, P.K., Tiwari, A.K., Singh, A.K., 2016. Risk assessment due to intake of metals in groundwater of east bokaro coalfield, Jharkhand, India. *Expo. Heal* 8, 265–275. <https://doi.org/10.1007/s12403-016-0201-2>.
- Mineral Resources Department 2014. <http://chhattisgarhminerals.gov.in/sites/default/files/treasure-trove-cg-minerals.pdf>.
- Mohammadi, A.A., Zarei, A., Majidi, S., Ghaderpoury, A., Hashempour, Y., Saghi, M.H., Alinejad, A., Yousefi, M., Hosseingholizadeh, N., Ghaderpoori, M., 2019. Carcinogenic and non-carcinogenic health risk assessment of heavy metals in drinking water of Khorramabad, Iran. *MethodsX* 6, 1642–1651. <https://doi.org/10.1016/j.mex.2019.07.017>.
- Mondal, N.C., Singh, V.S., Puranik, S.C., Singh, V.P., 2010. Trace element concentration in groundwater of Pesarlanka Island, Krishna Delta, India. *Environ. Monit. Assess.* 163, 215–227. <https://doi.org/10.1007/s10661-009-0828-6>.
- Norris, G., Duvall, R., Brown, S., Bai, S., 2014. *Epa Positive Matrix Factorization (Pmf) 5.0 Fundamentals and User Guide Prepared for the US Environmental Protection Agency Office of Research and Development*. Inc., Washington, dc.
- Paatero, P., 1997. Least squares formulation of robust non-negative factor analysis. *Chemometr. Intell. Lab. Syst.* 37, 23–35.
- Pandey, P.K., Sharma, R., Roy, M., Roy, S., Pandey, M., 2006. Arsenic contamination in the Kanker district of central-east India: geology and health effects. *Environ. Geochem. Health* 28, 409–420. <https://doi.org/10.1007/s10653-005-9039-4>.
- Prasanth, S.V.S., Magesh, N.S., Jitheshlal, K.V., Chandrasekar, N., Gangadhar, K., 2012. Evaluation of groundwater quality and its suitability for drinking and agricultural use in the coastal stretch of Alappuzha District, Kerala, India. *Appl. Water Sci.* 2, 165–175.
- Rahman, M.M., Naidu, R., Bhattacharya, P., 2009. Arsenic contamination in groundwater in the Southeast Asia region. *Environ. Geochem. Health* 31, 9–21. <https://doi.org/10.1007/s10653-008-9233-2>.
- Ravindra, K., Mor, S., 2019. Distribution and health risk assessment of arsenic and selected heavy metals in Groundwater of Chandigarh, India. *Environ. Pollut.* 250, 820–830. <https://doi.org/10.1016/j.envpol.2019.03.080>.
- Rubina, S., Kavita, T., 2013. *International journal of Research in advent technology*. Monitoring of fluoride contamination in southern region of Chhattisgarh, India: correlation with physico-chemical parameters international journal of Research in advent technology. *Int. J. Res. Advent Technol.* 1.
- Sethy, S.N., Syed, T.H., Kumar, A., Sinha, D., 2016. Hydrogeochemical characterization and quality assessment of groundwater in parts of Southern Gangetic Plain. *Environ. earth Sci.* 75, 232.

- Singh, G., Kamal, R.K., 2017. Heavy metal contamination and its indexing approach for groundwater of Goa mining region, India. *Appl. Water Sci.* 7, 1479–1485. <https://doi.org/10.1007/s13201-016-0430-3>.
- Sinha, M.K., 2011. *Ethnobotany in Relation to Health and Livelihood Security in District Bastar of Chhattisgarh State*. Raipur.
- US-EPA, 2014. EPA Positive Matrix Factorization (PMF) 5.0 Fundamentals and 136.
- US Environmental Protection Agency, 2011. *Exposure Factors Handbook: 2011 Edition*. U.S. Environ. Prot. Agency EPA/600/R.
- USEPA, 2004. *Risk Assessment Guidance for Superfund (RAGS). Volume I. Human Health Evaluation Manual (HHEM). Part E. Supplemental Guidance for Dermal Risk Assessment*.
- Varghese, J., Jaya, D.S., 2014. Metal pollution of groundwater in the vicinity of Valiathura sewage farm in Kerala, South India. *Bull. Environ. Contam. Toxicol.* 93, 694–698.
- Wang, C.H., Hsiao, C.K., Chen, C.L., Hsu, L.I., Chiou, H.Y., Chen, S.Y., Hsueh, Y.M., Wu, M.M., Chen, C.J., 2007. A review of the epidemiologic literature on the role of environmental arsenic exposure and cardiovascular diseases. *Toxicol. Appl. Pharmacol.* 222, 315–326. <https://doi.org/10.1016/j.taap.2006.12.022>.
- WHO, 2019. *Drinking-water*. <https://www.who.int/news-room/fact-sheets/detail/drinking-water>.
- Yavar Ashayeri, N., Keshavarzi, B., 2019. Geochemical characteristics, partitioning, quantitative source apportionment, and ecological and health risk of heavy metals in sediments and water: a case study in Shadegan Wetland, Iran. *Mar. Pollut. Bull.* 149, 110495. <https://doi.org/10.1016/j.marpolbul.2019.110495>.